Stanford Exploration Project, Report 110, September 18, 2001, pages 1–102

Born-compliant image perturbation for wave-equation migration velocity analysis

Paul Sava and Biondo Biondi[1]

ABSTRACT

Wave-equation migration velocity analysis produces wrong results if it starts from an image perturbation which is not compliant with the assumed Born approximation. Earlier attempts to correct this problem lead to either unreliable or hard to implement solutions. In this paper, we present a new method designed to construct image perturbations that are always compliant with the Born approximation. This new method is robust, easy to implement, and produces results that are consistent with those obtained using the ideal operators.

INTRODUCTION

The fundamental idea of wave-equation migration velocity analysis (WEMVA) is that we can establish a *linear* relation between a small perturbation in the slowness field and the corresponding perturbation in the image. Therefore, given an image perturbation, we can invert for the slowness perturbation.

The main challenge of WEMVA is to construct a correct image perturbation that can be inverted for slowness. This image need not be fully accurate, but ought to provide the correct *direction* and *magnitude* of the change.

In our early tests (Sava and Biondi, 2000), we construct the image perturbation using Prestack Stolt Residual Migration (PSRM) (Stolt, 1996; Sava, 2000). In summary, this residual migration method provides updated images for new velocity maps that correspond to a fixed ratio of the new velocity with respect to the original velocity map.

The main disadvantage of building the image perturbation using PSRM is that, if the velocity ratio parameter (γ) is too large, there is a good chance for the reference and the updated images to get out of phase. In other words, a large change in velocity violates the Born approximation. The end result is that the image perturbation computed by the forward operator and the one computed by residual migration are fundamentally different, and can have contradictory behaviors when using the Born WEMVA operator for inversion.

In previous reports, we have presented various attempts to solve this problem. All these attempts were related one way or another to the idea of scaling down the change in the γ

[1]**email:** paul@sep.stanford.edu, biondo@sep.stanford.edu

map, thus obeying the Born approximation, followed by scaling up of the inverted slowness map. Although these approaches were successful in several examples, none of them addressed the fundamental problem: does the (scaled) image perturbation created by residual migration match the one obtained by the forward WEMVA operator? Furthermore, scaling and rescaling cannot lead to a robust method, since they involve ad hoc processes and since the inversion problem we are trying to address is already highly nonlinear.

In this paper, we present a new method that can be used to create image perturbations for WEMVA. The two main goals here are

- to create an image perturbation that is compatible with the one computed using the forward WEMVA operator, and
- to create the image perturbation directly from the background image, and therefore compliant with the Born approximation.

We begin with a discussion of the WEMVA scattering operator, and continue with the derivation of our new method. Next we show a complex synthetic example and provide a discussion of the future work and of the problems that are still unsolved.

IMAGE PERTURBATION BY WEMVA

In migration by downward continuation, the wavefield at depth $z+\Delta z$ ($\mathcal{W}_{z+\Delta z}$) is obtained by phase-shift from the wavefield at depth z ($\mathcal{W}_z$)

$$\mathcal{W}_{z+\Delta z} = \mathcal{W}_z e^{-ik_z \Delta z}, \tag{1}$$

where the depth wavenumber k_z depends linearly through a Taylor series expansion on its value in the reference medium (${k_z}^o$) and the slowness in the depth interval from z to $z+\Delta z$, $s_o(z)$ and $s(x,y,z)$:

$$k_z \approx {k_z}^o + \left.\frac{dk_z}{ds}\right|_{s=s_o} \Delta s, \tag{2}$$

where, by definition, $\Delta s = s - s_o$.

If we denote the wavefield downward continued through the reference velocity as $\mathcal{W}^o_{z+\Delta z}$

$$\mathcal{W}^o_{z+\Delta z} = \mathcal{W}_z e^{-i{k_z}^o \Delta z}, \tag{3}$$

we obtain

$$\mathcal{W}_{z+\Delta z} = \mathcal{W}^o_{z+\Delta z} e^{-i \left.\frac{dk_z}{ds}\right|_{s=s_o} \Delta s \Delta z}. \tag{4}$$

The Born approximation linearizes the phase-shift exponential ($e^x \approx 1+x$), such that we can write

$$\mathcal{W}_{z+\Delta z} \approx \mathcal{W}^o_{z+\Delta z} - i\,\mathcal{W}^o_{z+\Delta z} \left.\frac{dk_z}{ds}\right|_{s=s_o} \Delta s \Delta z. \tag{5}$$

Therefore, at any particular depth level, the wavefield perturbation $\Delta \mathcal{W}$ is

$$\Delta \mathcal{W} \approx -i \Delta z \mathcal{W} \left. \frac{dk_z}{ds} \right|_{s=s_o} \Delta s, \tag{6}$$

which we can also write as

$$\boxed{\Delta \mathcal{W} \approx \frac{d\mathcal{W}}{dk_z} \left. \frac{dk_z}{ds} \right|_{s=s_o} \Delta s.} \tag{7}$$

The image perturbation is simply obtained from the wavefield perturbation by summation over frequencies:

$$\Delta \mathcal{R} = \sum_{\omega} \Delta \mathcal{W}. \tag{8}$$

IMAGE PERTURBATION BY RESIDUAL MIGRATION

Residual migration can also be used to create an image perturbation. In its simplest form, we can build it as a difference between an *improved* image ($\mathcal{R}$) and the *reference* image ($\mathcal{R}_o$)

$$\Delta \mathcal{R} = \mathcal{R} - \mathcal{R}_o, \tag{9}$$

where $\mathcal{R}$ is derived from $\mathcal{R}_o$ as a function of the parameter γ, which is the ratio of the original and improved velocities (Sava, 2000). Of course, the improved velocity map is unknown explicitly, but it is described indirectly by the ratio map of the two velocities.

If we define $\Delta \gamma = \gamma - 1$, we can also write the discrete version of the image perturbation as

$$\Delta \mathcal{R} \approx \frac{\mathcal{R} - \mathcal{R}_o}{\gamma - 1} \Delta \gamma, \tag{10}$$

equation which can be written in differential form as

$$\Delta \mathcal{R} \approx \left. \frac{d\mathcal{R}}{d\gamma} \right|_{\gamma=1} \Delta \gamma, \tag{11}$$

or, equivalently, using the chain rule, as

$$\boxed{\Delta \mathcal{R} \approx \frac{d\mathcal{R}}{dk_z} \left. \frac{dk_z}{d\gamma} \right|_{\gamma=1} \Delta \gamma,} \tag{12}$$

where k_z is the depth wavenumber defined for PSRM.

The Equations (7) and (12) are very similar, which comes at no surprise since they effectively represent the same thing: the perturbation of the image given a perturbation of the slowness field, or equivalently, a perturbation of the γ (ratio) field. We will use Equation (12) to create the image perturbation, which we will then backproject in the slowness space using the adjoint of the WEMVA equation (7).

Equation (12) offers the possibility to build the image perturbation directly. We achieve this by computing three elements: the derivative of the image with respect to the depth wavenumber, and two weighting functions, one for the derivative of the depth wavenumber with respect to the velocity ratio parameter (γ), and the other one for the magnitude of the $\Delta\gamma$ perturbation from the reference to the improved image.

Firstly, the image derivative in the Fourier domain, $\frac{d\mathcal{R}}{dk_z}$, is straightforward to compute in the space domain as

$$\left.\frac{d\mathcal{R}}{dk_z}\right|_{\gamma=1} = -iz\mathcal{R}_o. \tag{13}$$

The derivative image is nothing but the imaginary part of the migrated image, scaled by depth.

Secondly, we can obtain the weighting representing the derivative of the depth wavenumber with respect to the velocity ratio parameter, $\left.\frac{dk_z}{d\gamma}\right|_{\gamma=1}$, starting from the double square root (DSR) equation written for prestack Stolt residual migration (Sava, 2000):

$$\begin{aligned} k_z &= {k_z}^s + {k_z}^r \\ &= \frac{1}{2}\sqrt{\gamma^2\mu^2 - |\mathbf{k}_s|^2} + \frac{1}{2}\sqrt{\gamma^2\mu^2 - |\mathbf{k}_r|^2}, \end{aligned}$$

where μ is given by the expression:

$$\mu^2 = \frac{\left[4\left({k_z}^o\right)^2 + \left(|\mathbf{k}_r| - |\mathbf{k}_s|\right)^2\right]\left[4\left({k_z}^o\right)^2 + \left(|\mathbf{k}_r| + |\mathbf{k}_s|\right)^2\right]}{16\left({k_z}^o\right)^2}. \tag{14}$$

The derivative of k_z with respect to γ is

$$\frac{dk_z}{d\gamma} = \gamma\left(\frac{\mu^2}{4{k_z}^s} + \frac{\mu^2}{4{k_z}^r}\right), \tag{15}$$

therefore

$$\left.\frac{dk_z}{d\gamma}\right|_{\gamma=1} = \frac{\mu^2}{2\sqrt{\mu^2 - |\mathbf{k}_s|^2}} + \frac{\mu^2}{2\sqrt{\mu^2 - |\mathbf{k}_r|^2}}. \tag{16}$$

Finally, $\Delta\gamma$ can be picked from the set of residually migrated images at various values of the parameter γ (Sava, 2000). The main criterion that should be used is the flatness of the angle-domain image gathers, although in principle other derived parameters, such as stack power or semblance, can be used as well.

EXAMPLES

In this section, we demonstrate the method on a synthetic example. The reflectivity model (Figure 1) consists of two flat reflectors surrounding a set of reflectors dipping at 45 degrees.

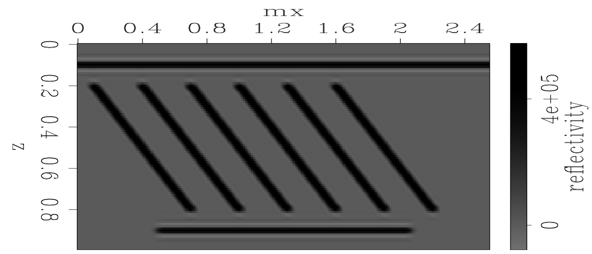

Figure 1: Reflectivity model. paul1-rr [ER]

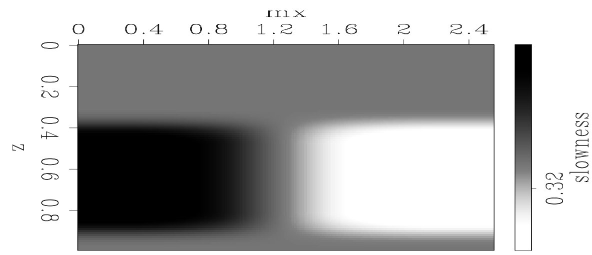

Figure 2: Background slowness model. paul1-s1 [ER]

The background velocity (Figure 2) is characterized by strong lateral variation to provide a somewhat complex background wavefield. The image perturbation (Figure 3) consists of a rectangular block in the upper part of the section, which creates perturbations in the image both on the flat and on the dipping reflectors. We change the magnitude of this anomaly from small values that satisfy the Born approximation, to high values that clearly violate the linear assumptions.

Figure 3: Slowness perturbation. paul1-ds [ER]

We use the true slowness to model the data, and then we use the background slowness to obtain the reference image and the reference wavefield. From the slowness perturbation, we use the forward WEMVA operator to create the *ideal* image perturbation (Figure 4). Backprojection by the adjoint WEMVA operator gives the slowness update in Figure 5, and inversion gives the slowness in Figure 6. Figures 4 and 5 represent the benchmark against which we want to compare our new image perturbation method.

Figure 7 represents the image perturbation created using Equation (12) where we consider that $\Delta\gamma = 1$. Of course, this is not our image perturbation, but it only gives us a rough idea of how we should pick the actual perturbation from after weighting with $\Delta\gamma$. As expected, the magnitude of this component of the image increases with depth.

Next we multiply the image in Figure 7 with the $\Delta\gamma$ weight (Figure 8) and obtain an image perturbation (Figure 9) which is comparable in shape and magnitude with the ideal perturbation (Figure 4). Backprojection by the adjoint WEMVA operator gives the slowness update in Figure 10, and inversion gives the slowness in Figure 11.

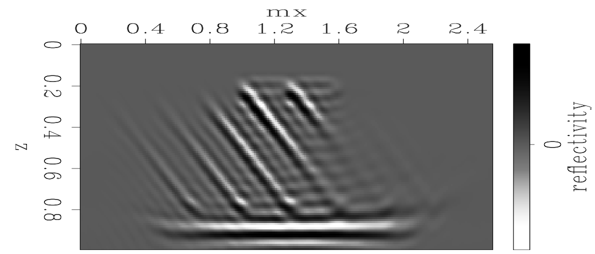

Figure 4: Ideal image perturbation obtained by the forward WEMVA operator. paul1-di.wei.01 [ER]

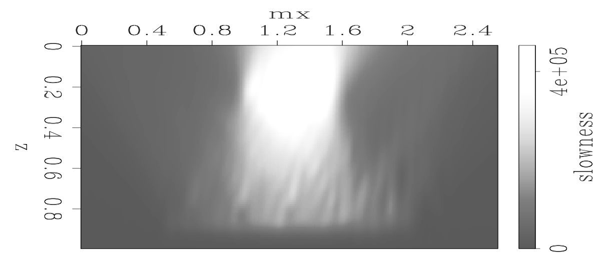

Figure 5: Slowness backprojection obtained from the ideal image perturbation using the adjoint WEMVA operator. paul1-bds.wei.01 [ER]

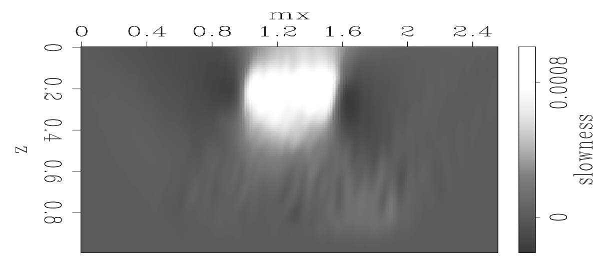

Figure 6: Slowness inversion obtained from the ideal image perturbation using the WEMVA operator. paul1-ids.wei.01 [ER]

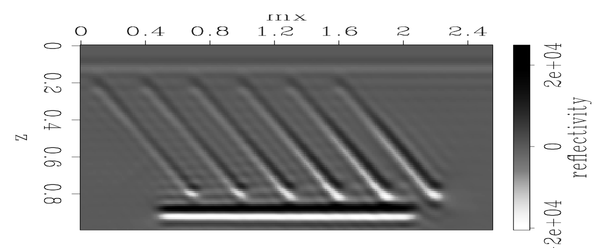

Figure 7: Image perturbation produced by Equation (12). The magnitude of the perturbation increases with depth. paul1-di.ana.full [ER]

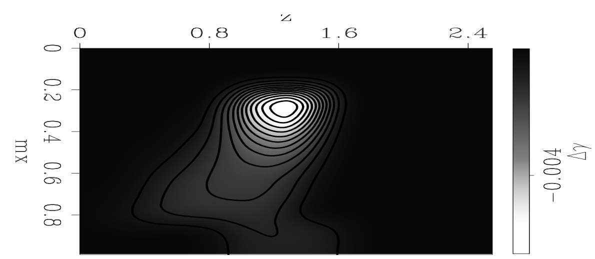

Figure 8: $\Delta\gamma$ in Equation (12). paul1-mask [ER]

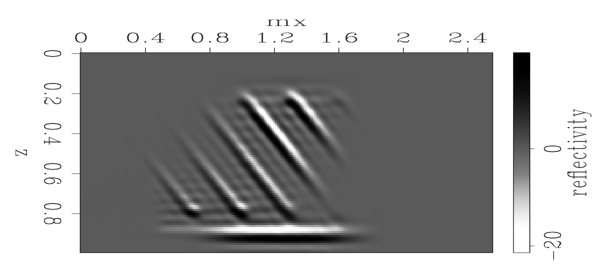

Figure 9: Analytical image perturbation obtained by multiplication of the image in Figure 7 with the weight in Figure 8. paul1-di.ana.01 [ER]

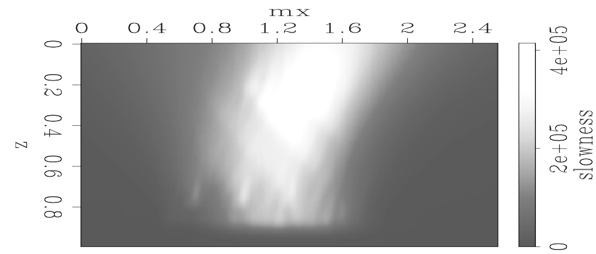

Figure 10: Slowness backprojection obtained from the analytical image perturbation using the adjoint WEMVA operator. paul1-bds.ana.01 [ER]

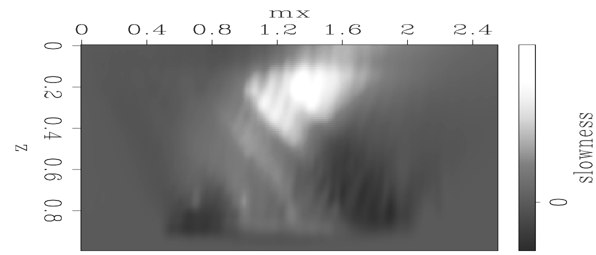

Figure 11: Slowness inversion obtained from the analytical image perturbation using the WEMVA operator. paul1-ids.ana.01 [ER]

Finally, Figures 12, 13, and 14 are comparisons of the various methods used to compute the image perturbation, and the corresponding slowness model. All figures are presented in landscape mode and have three columns and four rows.

- The first column contains the real part of the image perturbation ($\Delta\mathcal{R}$), the second column contains the slowness model (Δs) obtained using backprojection of the image perturbation, and the third column contains the inverted slowness model obtained from the same image perturbation.

- The first row represents $\Delta\mathcal{R}$ and Δs computed using the WEMVA forward and adjoint operators, the second row represents $\Delta\mathcal{R}$ and Δs in the case in which we narrow down the angular aperture in the image perturbation, the third row represents $\Delta\mathcal{R}$ and Δs of our new approach, and the fourth row represents $\Delta\mathcal{R}$ and Δs obtained using the PSRM method.

Each of the Figures 12, 13, and 14 corresponds to a different magnitude of the slowness anomaly, everything else remaining unchanged. The main comparison is between rows 2 and 3 of the composite image. We can observe that as we increase the magnitude of the anomaly, the shapes of $\Delta\mathcal{R}$ and Δs remain roughly unchanged, although the magnitudes of both the image and slowness perturbations increase. Since, by construction, we obey the Born approximation, we do not observe any out-of-phase effects.

In contrast, when we compare rows 3 and 4, that is our new method and the PSRM approach, we observe that, for the small anomalies, the image and slowness perturbations are very similar, but at high values of the anomaly, the PSRM $\Delta\mathcal{R}$ gets out of phase with respect to the background wavefield, and therefore the backprojected or inverted Δs either cancels or changes sign altogether. This is exactly the kind of effect we are trying to avoid using our new approach.

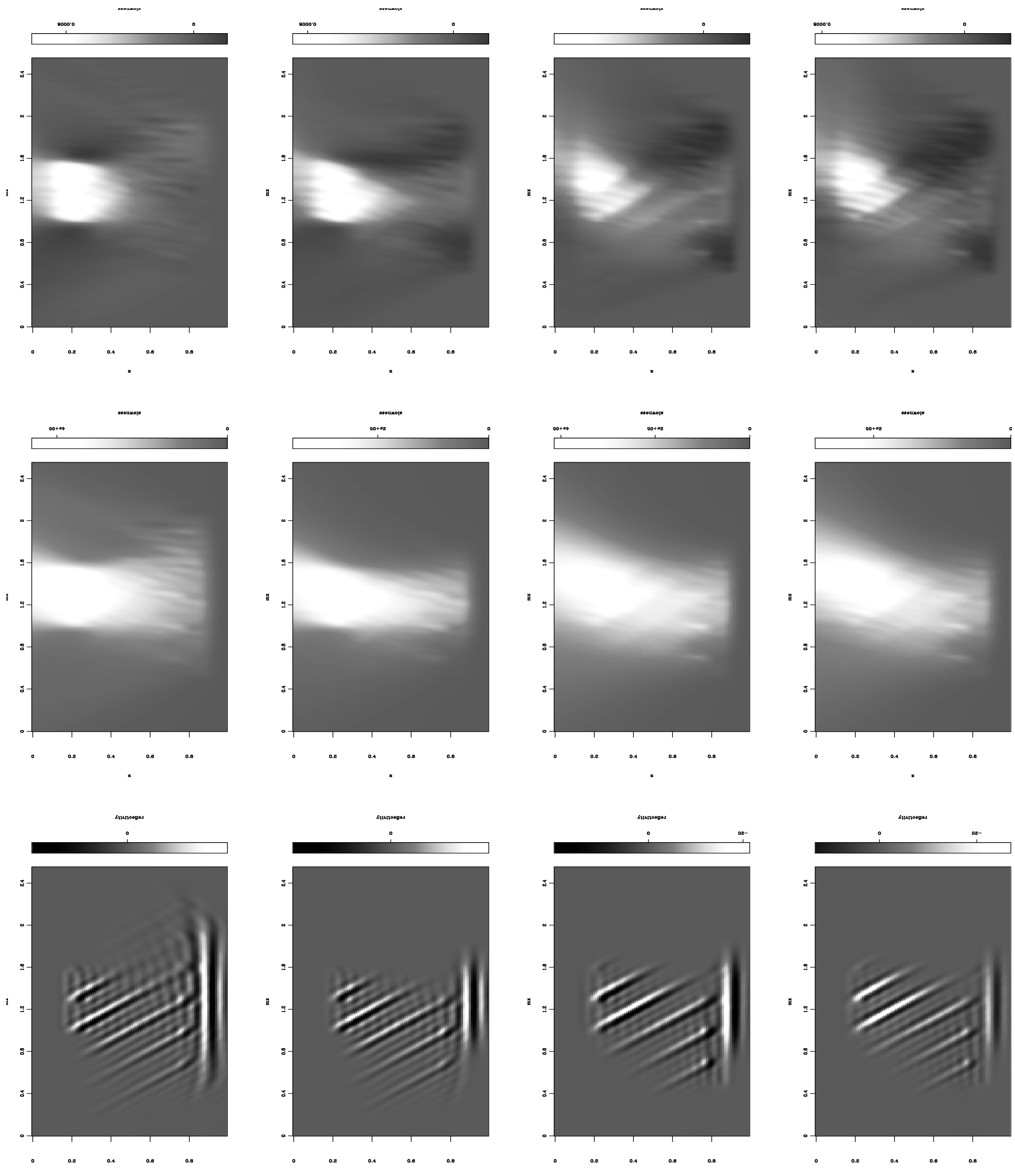

Figure 12: View as 4 rows and 3 columns. The left column represents the image perturbations, the middle represents backprojection using the WEMVA operator, and the right column represents unconstrained inversion in 3 iterations using the WEMVA operator. The top row is using the ideal image perturbation, the second row is using the narrow aperture image perturbation, the third row is using our new approach, and the fourth row the PSRM approach. paul1-block.01 [CR]

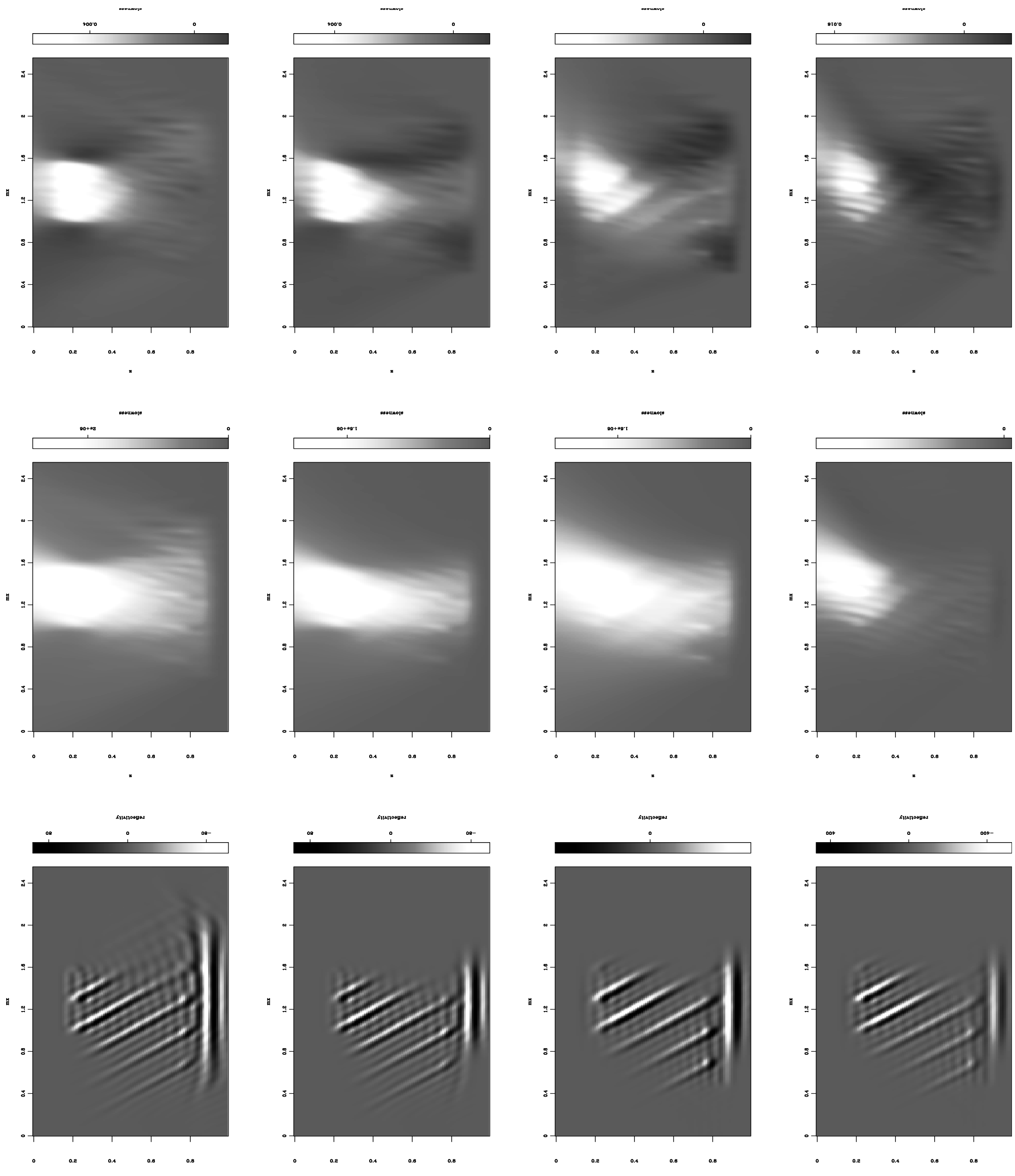

Figure 13: View as 4 rows and 3 columns. The left column represents the image perturbations, the middle represents backprojection using the WEMVA operator, and the right column represents unconstrained inversion in 3 iterations using the WEMVA operator. The top row is using the ideal image perturbation, the second row is using the narrow aperture image perturbation, the third row is using our new approach, and the fourth row the PSRM approach. paul1-block.06 [CR]

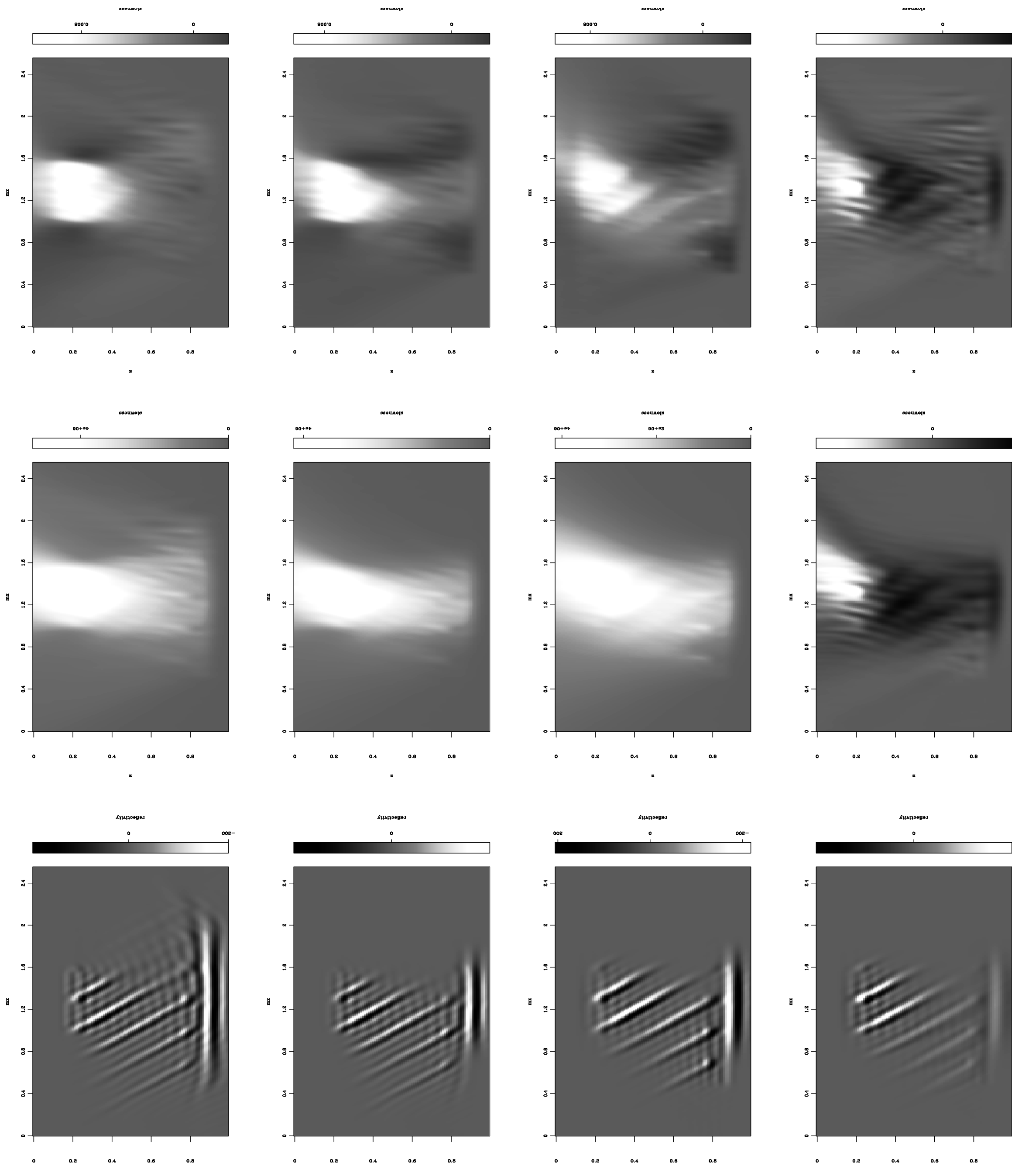

Figure 14: View as 4 rows and 3 columns. The left column represents the image perturbations, the middle represents backprojection using the WEMVA operator, and the right column represents unconstrained inversion in 3 iterations using the WEMVA operator. The top row is using the ideal image perturbation, the second row is using the narrow aperture image perturbation, the third row is using our new approach, and the fourth row the PSRM approach. paul1-block.11 [CR]

FUTURE WORK

At this moment, the main problem that is still not fully solved is that of picking the $\Delta\gamma$ (Figure 8) distribution. For the examples in this paper, we have artificially constructed this weight from information provided by the forward WEMVA operator, information which we would not normally have when dealing with real data.

In theory, this weight should be consistent with the flatness of the image gathers: smaller values for nearly flat events in the image gathers, and larger ones for events with higher moveout. As we mentioned earlier, we could use other parameters related to this moveout, such as stack power or semblance. In practice, however, any one of these approaches requires picking, which is a very tedious task, especially in 3-D. Perhaps, some kind of automatic picking (Clapp, 2001) is the answer, but this issue remains to be solved in future work.

CONCLUSIONS

We have presented a new approach to the construction of image perturbations for velocity analysis using WEMVA. This method directly constructs the image perturbation from the background image, and is always compliant with the Born approximation which is the underlying assumption of WEMVA. We show that, given correct scaling, we can obtain slowness anomalies that are fully consistent with those obtained by the application of the forward and adjoint WEMVA operators.

REFERENCES

Clapp, R., 2001, Ray-based tomography with limited picking: SEP–**110**, 103–112.

Sava, P., and Biondi, B., 2000, Wave-equation migration velocity analysis: Episode II: SEP–**103**, 19–47.

Sava, P., 2000, Prestack Stolt residual migration for migration velocity analysis: 70th Ann. Internat. Mtg., Soc. Expl. Geophys., Expanded Abstracts, 992–995.

Stolt, R. H., 1996, Short note–a prestack residual time migration operator: Geophysics, **61**, no. 02, 605–607.